Design of Peptidyl Compounds That Affect β-Amyloid Aggregation: Importance of Surface Tension and Context†

Todd J. Gibson and Regina M. Murphy*

Department of Chemical and Biological Engineering, University of Wisconsin, 1415 Engineering Drive, Madison, Wisconsin 53706

Received February 7, 2005; Revised Manuscript Received April 28, 2005

ABSTRACT: Self-association of β-amyloid (Aβ) peptide into cross-β-sheet fibrils induces cellular toxicity in vitro and is linked with progression of Alzheimer's disease. Previously, we demonstrated that hybrid peptides, containing a recognition domain that binds to Aβ and a disrupting domain consisting of a chain of charged amino acids, inhibited Aβ-associated toxicity in vitro and increased the rate of Aβ aggregation. In this work we examine the design parameter space of the disrupting domain. Using KLVFFKKKKKK as a base case, we tested hybrid compounds with a branched rather than linear lysine oligomer, with L-lysine replaced by D-lysine, and with lysine replaced by diaminopropionic acid. We synthesized a compound with a novel anionic disrupting domain that contained cysteine thiols oxidized to sulfates, as well as other compounds in which alkyl or ether chains were appended to KLVFF. In all cases, the hybrid compound's ability to increase solvent surface tension was the strongest predictor of its effect on Aβ aggregation kinetics. Finally, we investigated the effects of arginine on Aβ aggregation. Arginine is a well-known chaotrope but increases surface tension of water. Arginine modestly decreased Aβ aggregation. In contrast, RRRRRR slightly, and KLVFFRRRRRR greatly, increased Aβ aggregation. Thus, the influence of arginine on Aβ aggregation depends strongly on the context in which it is presented. The effect of arginine, RRRRRR, and KLVFFRRRRRR on Aβ aggregation was examined in detail using laser light scattering, circular dichroism spectroscopy, Fourier transform infrared spectroscopy, thioflavin T fluorescence, and transmission electron microscopy.

Amyloid fibril formation is linked to several neurodegenerative disorders including Alzheimer's disease (AD).[1] In AD, β-amyloid (Aβ), a 40−43 residue long peptide cleaved from the membrane-bound amyloid precursor protein APP, aggregates into cross-β-sheet fibrils. According to the amyloid cascade hypothesis, deposition of Aβ fibrils in brain tissue initiates a cascade of events leading to extensive neuronal cell death (*1*−*3*). Oligomeric intermediates in the Aβ aggregation pathway may be more toxic than the final fibrillar deposits (*4*−*10*). In agreement with this hypothesis, we observed that synthetic peptides that accelerate Aβ aggregation protect against Aβ toxicity (*11*−*13*), presumably by accelerating association of soluble oligomers into fully formed fibrils and thereby reducing the concentration of putative toxic intermediates. The effective peptides were hybrid compounds, containing KLVFF as a recognition domain to provide binding specificity, linked to a chain of charged amino acids, such as KKKKKK or EEEE, that act as a disrupting domain.

In work reported here, we explore the diversity possible in design of the disrupting domain. KLVFFKKKKKK serves as our base case compound. We test the effect on hybrid compound activity of (a) a branched rather than linear display of the lysine oligomer, (b) substitution of D-lysine for L-lysine, and (c) replacement of the long lysine side chain [$-(CH_2)_4NH_3^+$] with the shorter diaminopropionate side chain ($-CH_2NH_3^+$). Previously, we showed that a derivatized hybrid peptide, in which cationic betaine was incorporated into the lysine side chains of the disrupting domain, accelerated Aβ aggregation far more than any other compound (*14*). Here we extend this work by synthesis and testing of hybrid compounds in which the oligomeric lysine is replaced with a derivatized anionic disrupting domain and with alkyl or ether chains. With all test compounds, we observe a strong positive correlation between surface tension increase and Aβ aggregation acceleration.

Betaine is categorized as a strong Hofmeister kosmotrope (Figure 1), a cosolute tending to stabilize protein structure (*15*, *16*). Kosmotropes are believed to affect folded protein stability predominantly through a preferential exclusion mechanism, a phenomenon that also accounts for the kosmotrope's tendency to increase solvent surface tension. Indeed, the effectiveness of a kosmotrope at stabilizing protein structure generally correlates with its ability to

† This work was supported by National Institutes of Health Grant NS 37728.

* Corresponding author: e-mail, regina@engr.wisc.edu; phone, 608-262-1587; fax, 608-262-5434.

[1] Abbreviations: Aβ, β-amyloid; AD, Alzheimer's disease; ArgHCl, L-arginine monohydrochloride; Arg, L-arginine; Fmoc, fluorenylmethoxycarbonyl; Boc, *tert*-butoxycarbonyl; Ahx, aminohexanoic acid; Dpr, diaminopropionic acid; AEEA, aminoethoxyethoxyacetic acid; Mmt, 4-methoxytrityl; TFA, trifluoroacetic acid; HPLC, high-performance liquid chromatography; MALDI-TOF, matrix-assisted laser desorption/ionization time of flight; PBSA, phosphate-buffered saline with azide; DLS, dynamic light scattering; SLS, static light scattering; CD, circular dichroism; FTIR, Fourier transform infrared spectroscopy; ThT, thioflavin T; TEM, transmission electron microscopy.

10.1021/bi050225s CCC: $30.25
Published on Web 05/27/2005

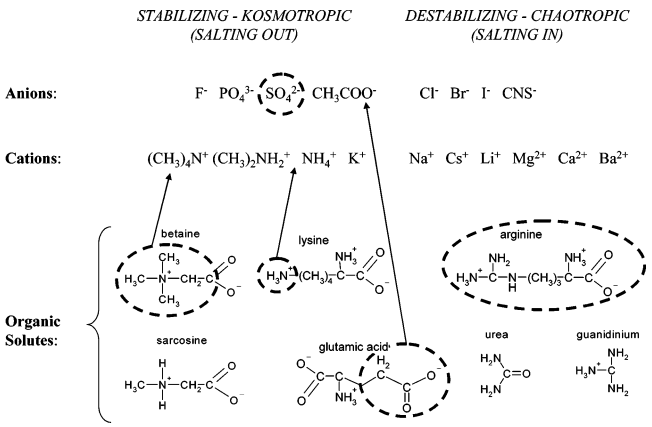

FIGURE 1: Hofmeister series (*16*). Ions and solutes are ranked, from left to right, according to their ability to stabilize structured protein. The location of the side chain groups of lysine, glutamic acid, and betaine are indicated in the kosmotrope ionic series.

increase solvent surface tension (*17*, *18*). We hypothesize that the observed correlation between increased surface tension and acceleration of Aβ aggregation is attributable to a preferential exclusion mechanism and that our hybrid compounds act as targeted kosmotropes: since the Aβ monomer lacks defined structure, aggregated Aβ is the more structured state and is therefore stabilized. The Hofmeister series also includes a number of chaotropic cosolutes (Figure 1) that destabilize folded proteins. Their effect is likely due to preferential interactions between the chaotrope and the protein (*15*, *16*); unlike kosmotropes, the effect of chaotropes on protein stability does not generally correlate with solvent surface tension effects. Arginine is one example of a chaotropic cosolute that can destabilize folded protein. In particular, arginine has been shown to destabilize incorrectly folded proteins (*19*) and/or enhance the solubility of aggregation-prone species (*20*), leading to its utilization in many refolding schemes to suppress protein aggregation (*21*−*26*). We demonstrate very different consequences for Aβ aggregation when arginine is presented as a monomer or as an oligopeptide or appended as a disrupting domain to KLVFF. We further demonstrate the importance of multiple biophysical tools to fully characterize these effects. Results presented here are useful not only for delineation of the requirements for effective disrupting domains in Aβ aggregation modulators but also for elucidating the influence of cosolutes on protein stability and aggregation generally.

EXPERIMENTAL PROCEDURES

Peptides. L-Arginine monohydrochloride (ArgHCl) and L-arginine (Arg) were purchased from Sigma Aldrich (St. Louis, MO). Aβ(1−40) was purchased from Anaspec, Inc. (San Jose, CA). All other peptides were synthesized by Fmoc solid-phase peptide synthesis with the use of an Applied Biosystems (Foster City, CA) Model 432A "Synergy" automated synthesis instrument. Protected natural amino acids, aminohexanoic acid (Ahx), diaminopropionic acid (Dpr), and resins were purchased from Novabiochem (La Jolla, CA). Aminoethoxyethoxyacetic acid (AEEA) was purchased from Applied Biosystems. One modified peptide, compound **2** (Table 1), required additional synthesis procedures. First, KLVFFCCCE was synthesized on a Wang resin, with 4-methoxytrityl (Mmt) protection on the cysteine side

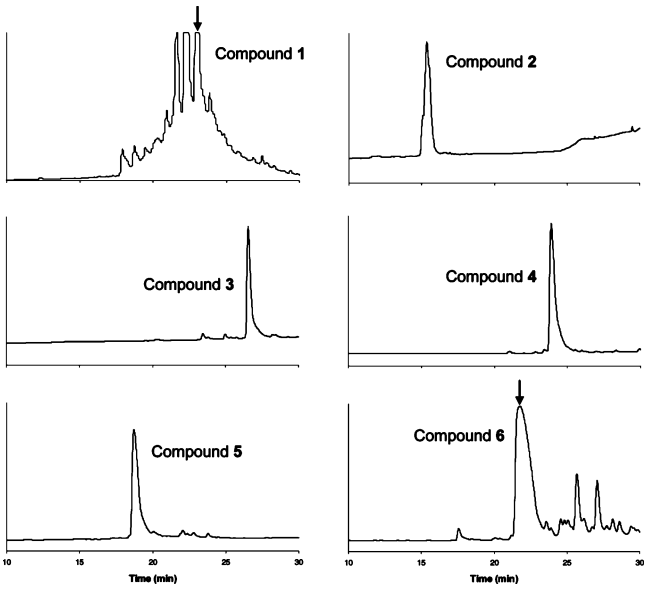

FIGURE 2: Structure and reverse-phase HPLC chromatogram of crude compounds. The compounds were purified by collecting the peak corresponding to the desired product, as confirmed by MALDI-TOF mass spectroscopy analysis (Table 1); for compounds **1** and **6**, the collected peak is indicated with an arrow.

chains. Performic acid [1:19 (v/v) 30% H_2O_2:88% formic acid] was added to KLVFFCCCE (while still on the resin) on dry ice to achieve cleavage of the Mmt groups and subsequent oxidation of the cysteine thiols to sulfates. For the synthesis of compound **6** (Table 1), all lysines, except the carboxy-terminal lysine, contained Fmoc side chain protection (instead of Boc protection) so that coupling to each lysine side chain in addition to each lysine N-terminus was achieved. After synthesis was complete, peptide resins were washed with ethanol and dried. Resin cleavage was accomplished with 95% TFA, and the resulting peptides were precipitated and washed with diethyl ether. The cleaved peptides were purified by reverse-phase HPLC (C4 column) using an acetonitrile/water gradient (Figure 2). Fractions were collected and analyzed by MALDI-TOF mass spectrometry (Table 1). Purified peptides were stored as lyophilized powders at −70 °C.

Light Scattering. The rate of Aβ aggregation and the size of aggregates were monitored with dynamic light scattering (DLS) and static light scattering (SLS). First, 10 mL of 8 M urea in glycine−NaOH buffer (0.1 M, pH 10) was prepared and filtered with a 0.22 μm Millipore Millex GV sterilized filter. Then ∼1 mL of the filtered 8 M urea was filtered a second time with a fresh Millex GV 0.22 μm sterile filter. The same filtration procedure was used for phosphate-buffered saline with azide [PBSA; 0.01 M Na_2HPO_4/NaH_2PO_4, 0.15 M NaCl, 0.02% (w/v) NaN_3, pH 7.4], except that ∼70 mL of PBSA was filtered first and then ∼3.5 mL was filtered in the second filtration step. Test compounds were dissolved directly into double-filtered PBSA. Aβ was dissolved in double-filtered 8 M urea at 2.8 mM for 10 min to ensure solubilization and disruption of any preformed aggregates or secondary structure, and this solution was then diluted 20-fold into double-filtered PBSA or PBSA containing test compound. Each sample contained 140 μM Aβ with 140 μM hybrid compound, 140 μM RRRRRR, 5.7 mM Arg, or 5.7 mM ArgHCl. All samples (except Arg) were at pH 7.4 and contained 0.4 M urea. Samples were quickly filtered

Table 1: Hybrid Compounds[a]

Compound	Structure	Expected/Measured Molecular Mass (Da)
1	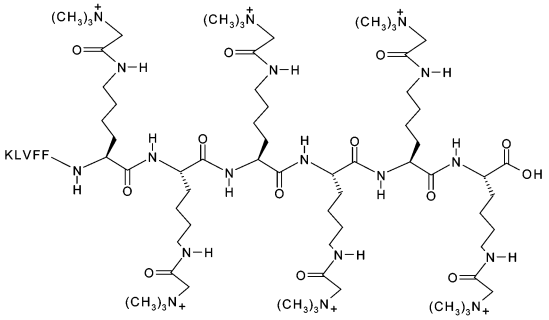	2017/2012
2	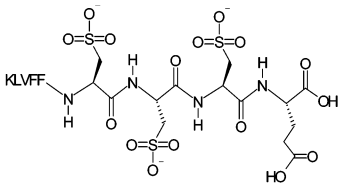	1237/1235
3	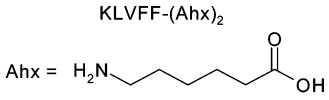	879/879
4	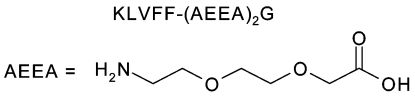	1000/1000
5	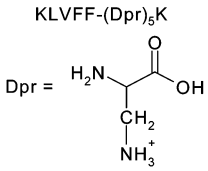	1211/1211
6	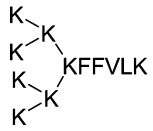	1551/1549

[a] Molecular masses of purified hybrid compounds were determined by MALDI-TOF mass spectrometry (MS).

through Millex HV 0.45 μm filters directly into clean light scattering cuvettes. DLS data at 90° scattering angle as well as SLS data (20−135°) were collected using a Coherent (Santa Clara, CA) argon ion laser at 488 nm and a Malvern (Spring Lane, U.K.) 4700 system, as described in more detail elsewhere (*13*).

Surface Tension. The equilibrium surface tension of hybrid compound solutions was measured using a FTÅ200 pendant drop tensiometer (First Ten Angstroms, Portsmouth, VA). Hybrid compounds were dissolved at concentrations ranging from 140 to 420 μM in double-filtered PBSA that was prepared identically to the PBSA used in light scattering experiments. Double-filtered 8 M urea (prepared as for light scattering experiments) was then added to double-filtered PBSA, or PBSA containing the hybrid compounds, to give a final urea concentration of 0.4 M. A droplet of the resulting solution was then formed at the end of a blunt, 22-gauge stainless steel needle, and the shape of the droplet was imaged. The surface tension was measured by fitting the Young−Laplace equation to the contour of drop shape once equilibrium was reached. Surface tension values were determined as the average of duplicate measurements.

In measuring the effects of hybrid compounds on solvent surface tension, solutions of hybrid compounds were prepared in the same solvent (0.4 M urea in PBSA) that was utilized for aggregation studies. Unlike the aggregation studies, however, Aβ was not present when measuring surface tension. Because the hybrid compounds experience a different environment in the actual scenario of interest (with aggregating Aβ present), care had to taken when interpreting the surface tension measurements. In other words, a compound may change the surface tension of a 0.4 M urea solution differently than the same compound would change the surface tension of a solution containing 140 μM Aβ in 0.4 M urea. The surface tension of the control case for these two solutions is different; while 0.4 M urea in PBSA has a

surface tension of ~72 dyn/cm, we observed that the surface tension of a solution of 140 μM Aβ in this same solvent was ~52 dyn/cm. It was discovered serendipitously that filtration of the stock solutions used in preparation of the samples with 0.22 μm Millipore Millex GV sterilized filters reduced the surface tension of the solvent to ~52 dyn/cm, presumably due to leaching of adsorbed gases used during filter manufacture. This effect was reproducible but diminished if larger volumes of solution were filtered. Hence, by including filtration of consistent volumes of stock solutions with sterile Millex filters in preparation of every hybrid compound sample, it was possible to determine the effect of hybrid compounds on the surface tension of a solution comparable in its initial-state surface tension to a solution of 140 μM Aβ.

Circular Dichroism (CD). The secondary structure of soluble Aβ was determined from circular dichroic spectra collected on an Aviv 62A DS circular spectrometer (Aviv Associates, Lakewood, NJ) in the far-UV range 210−260 nm. Samples of Aβ alone or with a test compound were prepared in an identical manner as samples for light scattering experiments. After 2 h, samples were placed in 1 mm path length quartz cells for measurement. The spectrum of the background was measured first and was subtracted from the sample spectrum. Test compound was included in the background for Arg and ArgHCl samples. The lower wavelength boundary was 210 nm due to the presence of urea. Spectra were not analyzed quantitatively for secondary structure due to lack of data below 210 nm.

Fourier Transform Infrared (FTIR) Spectroscopy. The secondary structure of precipitated Aβ aggregates was determined using Fourier transform infrared spectroscopy, performed on a Tensor 27 FT-IR spectrometer with an A529-P ATR attachment (Bruker Optics Inc., Billerica, MA). Aggregated samples used for light scattering or circular dichroism experiments were collected after several weeks of aggregation. After the samples were centrifuged at 16000*g* for 5 min, most of the supernatant was discarded. MilliQ H_2O (50 μL) was added to the pellet, and the samples were vortexed rapidly for 20 s. Samples were then lyophilized to remove all solvent. The remaining precipitate was placed on a ZnSe crystal surface and scanned from 1400 to 1800 cm^{-1} for amide I and amide II absorption.

Thioflavin T (ThT) Fluorescence. The amount of amyloid fibril available for binding in Aβ aggregate samples was determined by measuring ThT fluorescence. Samples of Aβ alone or with a test compound were prepared in an identical manner as samples for light scattering experiments, except (a) the final Millex HV 0.45 μm filtration step after dilution of the Aβ stock solution into PBSA was omitted and (b) samples were maintained at 37 °C during aggregation. A stock solution of 1 mM ThT in H_2O was prepared and filtered (Millex HV 0.45 μm) into a test tube, which was wrapped in aluminum foil and stored at 4 °C. Immediately before performing a ThT measurement, the stock solution was diluted 20-fold with filtered (Millex GV 0.22 μm) H_2O. Aggregate samples (10 μL) were added to each well of a 96-well plate, followed by 200 μL of diluted ThT solution. Fluorescence was measured with a BioTek Instruments, Inc. (Winooski, VT), FLx800 microplate fluorescence reader using an excitation wavelength of 440/30 nm and an emission wavelength of 485/20 nm.

Table 2: Effect of Hybrid Compounds on Aβ Aggregation and Solvent Surface Tension[a]

compound name	purpose of disrupting domain	effect on Aβ aggregation	effect on solvent surface tension
KLVFFKKKKKK	cationic kosmotrope	++	++
KLVFFEEEE	anionic kosmotrope	++	++
compound **1**	stronger cationic kosmotrope	+++	+++
compound **2**	stronger anionic kosmotrope	0	0
compound **3**	hydrophobic alkyl chain	0	0
compound **4**	ether chain	−	0
compound **5**	shorter side chain	+	+
compound **6**	branched lysine	0	+
KLVFFkkkkkk	stereochemistry	++	++
KLVFFRRRRRR	cationic chaotrope	+++	+++

[a] All hybrid compounds were dissolved in PBSA. To measure the effect on Aβ aggregation, compounds were mixed with Aβ (140 μM) at a 1:1 molar ratio and analyzed by light scattering. Surface tension effects were measured using the pendant drop method on solutions containing 140−420 μM test compound. Key: + to +++, increase to large increase; 0, little to no change; −, decrease.

Transmission Electron Microscopy (TEM). The morphology of Aβ aggregates was imaged using a Philips CM120 transmission electron microscope (FEI Corp., Eindhoven, The Netherlands). Aggregated samples used for light scattering or circular dichroism experiments were collected after 1−2 weeks of aggregation. After the samples were centrifuged at 16000*g* for 5 min, most of the supernatant was discarded. MilliQ H_2O (50 μL) was added to the remaining pellet, and the samples were vortexed rapidly for 20 s. Samples were stained with Nano-W (methylamine tungstate) negative stain (Nanoprobes.com, Yaphank, NY) and were placed on a pioloform coating grid support film (Ted Pella Inc., Redding, CA).

RESULTS

Hybrid peptides, comprised of a recognition domain of KLVFF and a disrupting domain of amino acids with charged side chains, accelerated Aβ aggregation and inhibited Aβ toxicity (*11*−*13*). One particularly effective hybrid peptide was KLVFFKKKKKK, with a chain of the cationic kosmotrope lysine (Figure 1) as its disrupting domain. We synthesized hybrid compounds with novel disrupting domains (Tables 1 and 2) to determine the influence of variations from the lysine hexamer design. Hybrid compounds were examined for their influence on Aβ (140 μM) aggregation using laser light scattering. The surface tension of solutions of the compounds in PBSA (in the absence of Aβ) was measured.

We first tested the importance of steric effects, stereochemistry, and side chain length of the disrupting domain. Using KLVFFKKKKKK as a base case, we examined a hybrid compound with L-lysine replaced by D-lysine (KLVFFkkkkkk), a hybrid compound with the long lysine side chain replaced by the shorter diaminopropionate (Dpr) side chain (compound **5**), and a hybrid compound with a branched rather than linear lysine oligomer disrupting domain (compound **6**). The effect of KLVFFkkkkkk on both Aβ aggregation and solvent surface tension was similar to that

of KLVFFKKKKKK; compounds **5** and **6** had less effect on both aggregation and surface tension (Table 2).

Betaine contains a substituted amine at its terminus, which is categorized by the Hofmeister series to be a stronger cationic kosmotrope than the primary amine of lysine (Figure 1). Appending betaine to the lysine side chains resulted in a novel hybrid compound, compound **1**, which increased by 50-fold the hydrodynamic diameter of Aβ aggregates, compared to KLVFFKKKKKK (*14*). In addition to KLVFF-KKKKKK and compound **1**, previous work demonstrated that KLVFFEEEE was effective at accelerating Aβ aggregation (*13*). KLVFFEEEE contains glutamic acid, an anionic kosmotrope (Figure 1), in its disrupting domain. On the basis of these results, we investigated whether incorporation of a stronger anionic kosmotrope would improve the performance of KLVFFEEEE. We chose to incorporate sulfate groups by fully oxidizing the cysteine thiol side chains of KLVFFC-CCE. The resulting compound, compound **2**, had almost no effect on Aβ aggregation (Table 2). Previously, we observed that compound **1**, besides greatly accelerating Aβ aggregation, also greatly increased surface tension of the aqueous solvent (*14*). The influence of kosmotropes on protein stability and/or aggregation generally correlates with their ability to increase solvent surface tension (*17*). In sharp contrast to compound **1**, compound **2** had little effect on the solvent surface tension. At a concentration of 140 μM, for example, compound **1** increased the surface tension of sterile-filtered PBSA containing 0.4 M urea from 52.2 $\pm$ 0.2 to 59 $\pm$ 1 dyn/cm, while compound **2** produced an increase to only 53.5 $\pm$ 0.5 dyn/cm.

These results indicate that surface tension effects may be more predictive of the influence of hybrid compounds on Aβ aggregation than the Hofmeister series. We examined two more hybrid compounds, **3** and **4**. It was anticipated that either the alkyl chain of **3** or the ether chain of **4** might decrease solvent surface tension. We observed that neither of these compounds had a significant effect on Aβ aggregation, with only a slight decrease in aggregation rate resulting from compound **4**, and that the compounds correspondingly had very little effect on solvent surface tension (Table 2). The data from all of these compounds can be summarized succinctly by noting that the ability to increase the solvent surface tension was a strong predictor of a hybrid compound's ability to accelerate Aβ aggregation (Table 2, Figure 3).

All hybrid compounds with charged disrupting domains in Table 2 and Figure 3 contain kosmotropic groups (according to the Hofmeister series) except one: KLVFFR-RRRRR. Although arginine is similar to lysine in that both have basic side chains, unlike lysine, arginine acts as a chaotrope toward many proteins. Chaotropic activity of arginine normally results in suppression of protein aggregation and is attributed to affinity of the guanidinium group for the protein backbone through hydrogen bonding (*27*) or through interactions with specific protein domains, such as aromatic amino acid side chains (*26*), thus preventing intermolecular interactions of protein hydrophobic regions (*20*). We initially hypothesized that KLVFFRRRRRR might behave in an opposite manner than other hybrid compounds, reducing the rate of Aβ aggregation because of arginine's chaotropic nature. However, KLVFFRRRRRR accelerated Aβ aggregation greatly, to levels comparable to the effect

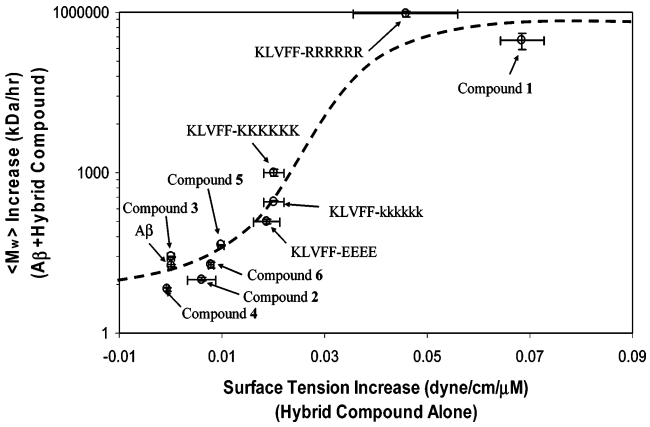

FIGURE 3: Correlation between surface tension increase of hybrid compounds (without Aβ present) and increase in weight-average molecular weight $\langle M \rangle_w$ of Aβ plus hybrid compounds (140:140 μM). The surface tension of hybrid compound solutions was measured using the pendant drop method at two or more concentrations (140−420 μM). The surface tension increase (*x*-axis) was determined by plotting surface tension versus concentration and obtaining the slope by linear regression. SLS measurements were collected several hours after initiation of aggregation, and the data were fit to determine $\langle M \rangle_w$, using methods described elsewhere (*34*). The increase in $\langle M \rangle_w$ (*y*-axis) was calculated as the measured $\langle M \rangle_w$ minus the molar mass of monomeric Aβ (4.3 kDa), divided by the number of hours the sample had been allowed to aggregate prior to SLS measurement.

of compound **1** (Figure 3). KLVFFRRRRRR also increased surface tension to similar levels as compound **1**, supporting the correlation between increase of Aβ aggregation rate and increase in surface tension observed for other hybrid compounds.

Given the marked activity of KLVFFRRRRRR, we chose to examine the effect of arginine on Aβ aggregation when arginine is presented in different contexts. We sought to determine if there would be a greater influence of chaotropic effects on Aβ aggregation in scenarios where the KLVFF recognition domain was not present. We tested the effects of arginine monomer [L-arginine (Arg) and L-arginine monohydrochloride (ArgHCl)] as well as arginine oligomer (RRRRRR) on aggregation of 140 μM Aβ. Arg and ArgHCl were both tested at a concentration of 5.7 mM ($\sim$40 times the molar equivalent of Aβ) because Arg increased the solvent surface tension at this concentration to similar levels as 140 μM KLVFFRRRRRR ($\sim$20% increase in surface tension). The salt form of arginine (ArgHCl) was examined because Arg changes the solvent pH, while the salt form does not. RRRRRR, which contains the standard, nonsalt form of L-arginine, was tested at an equimolar (140 μM) concentration to Aβ. At this concentration, RRRRRR increased surface tension by $\sim$5% and did not change the buffer pH.

RRRRRR resulted in an increase in intensity of scattered light, but not nearly to the level as the increase resulting from KLVFFRRRRRR (Figure 4A). The hydrodynamic diameter of Aβ aggregates increased nearly 15-fold after 4 h with RRRRRR present, compared to an increase of 140-fold with KLVFFRRRRRR present (Figure 4B). ArgHCl (pH 7.4) caused a slight reduction in scattered light intensity (Figure 4C), while the hydrodynamic diameter remained nearly unchanged (Figure 4D). Arg (pH 9.0) significantly decreased the scattered light intensity (Figure 4C) but

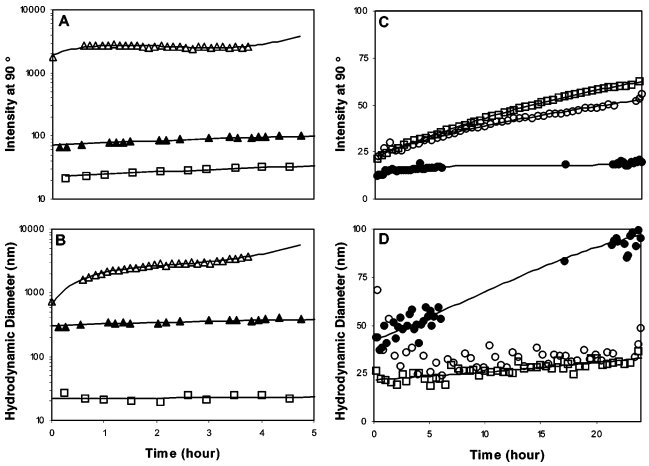

FIGURE 4: Aβ was dissolved in 8 M urea and then diluted 20-fold (to a final concentration of 140 μM) into PBSA alone (open square) or with 5700 μM ArgHCl (open circle), 5700 μM Arg (solid circle), 140 μM RRRRRR (solid triangle), or 140 μM KLVFFRRRRRR (open triangle). Growth was followed by dynamic light scattering. (A) Average scattered intensity for Aβ alone and in the presence of RRRRRR or KLVFFRRRRRR. (B) Average hydrodynamic diameter for Aβ alone and with RRRRRR or KLVFFRRRRRR as determined by cumulant analysis of autocorrelation data. (C) Average scattered intensity for Aβ alone and in the presence of Arg or ArgHCl. (D) Average hydrodynamic diameter for Aβ alone and with Arg or ArgHCl as determined by cumulant analysis of autocorrelation data.

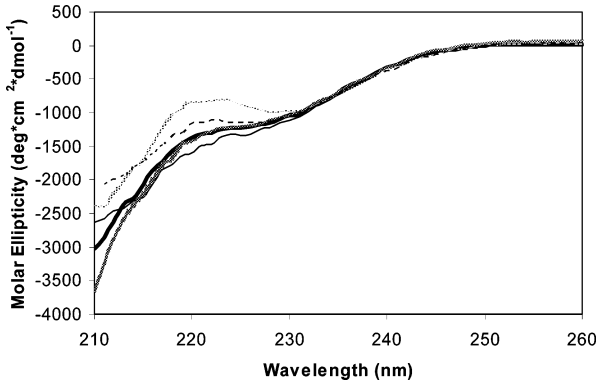

FIGURE 5: Aβ was dissolved in 8 M urea and then diluted 20-fold (to a final concentration of 140 μM) into PBSA alone (dark thin line) or with 140 μM RRRRRR (dashed line), 140 μM KLVFFRRRRRR (light thin line), 5700 μM ArgHCl (light thick line), or 5700 μM Arg (dark thick line). After 2 h, samples were placed in 1 mm path length quartz cells for circular dichroism spectrum measurement. The spectrum of the background was measured first and was subtracted from the sample spectrum. Test compound was included in the background for Arg and ArgHCl.

increased the hydrodynamic diameter of aggregates (Figure 4D). Since an increase in hydrodynamic diameter represents an increase in aggregate length while a decrease in scattering intensity represents a decrease in aggregate molar mass, these results indicate that fewer, but longer, aggregates form in the presence of Arg.

We further investigated and compared the influence of KLVFFRRRRRR, RRRRRR, ArgHCl, and Arg on Aβ aggregation by looking at the compounds' effects on aggregate secondary structure and morphology. CD measurements were taken ~2 h after sample preparation. None of the four test compounds had much effect on the ellipticity profile (Figure 5), indicating that there was little change in the degree of β-sheet structure present in soluble Aβ fractions. Similar ellipticity profiles were obtained after 24 h aggregation (data not shown) for Aβ alone or with ArgHCl or Arg present, which suggests that β-sheet structure was obtained early in the aggregation process and the degree of structure did not change significantly with time. As previously reported, no change in CD spectra was caused by peptides with intermediate effects on Aβ aggregation (i.e., KLVFFKKKKKK) (*33*).

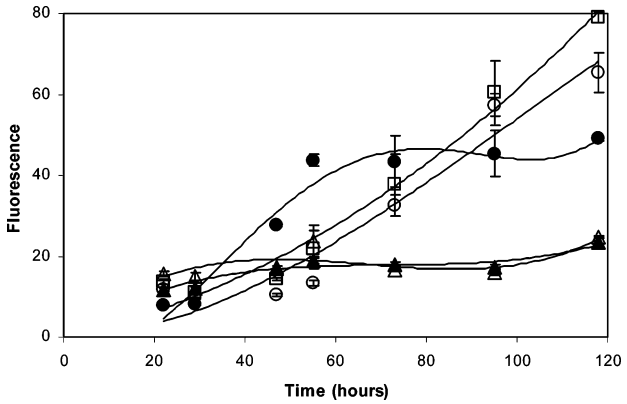

FIGURE 6: Aβ was dissolved in 8 M urea and then diluted 20-fold (to a final concentration of 140 μM) into PBSA alone (open square) or with 5700 μM ArgHCl (open circle), 5700 μM Arg (solid circle), 140 μM RRRRRR (solid triangle), or 140 μM KLVFFRRRRRR (open triangle). Samples were maintained at 37 °C during aggregation, and ThT fluorescence was measured at various time points with an excitation wavelength of 440 nm and an emission wavelength of 485 nm.

We also investigated whether the arginine-containing compounds were causing changes in β-sheet structure of fully aggregated material. To do so, we allowed samples to aggregate for several weeks, centrifuged the samples, recovered the precipitate, and collected FTIR spectra in the amide I stretching frequency region. The existence of a peak at ~1625 cm^{-1} was used as a marker for β-sheet structure (*28*, *29*). With RRRRRR or KLVFFRRRRRR present, the FTIR spectra were nearly identical to the spectra for Aβ alone (data not shown). With Arg or ArgHCl present, the peak at 1625 cm^{-1} was observed although there was a slight reduction in the relative size of the peak.

ThT fluorescence measurements were taken during aggregation of Aβ alone or with the arginine-containing compounds present to determine the amount of exposed amyloid fibril binding sites (Figure 6). For Aβ alone, the fluorescence increased with time, especially after 48 h of aggregation. ArgHCl had no effect on the ThT profile and Arg had a very modest effect. Interestingly, ThT fluorescence was absent in samples containing Aβ with either RRRRRR or KLVFFRRRRRR, despite the acceleration in aggregation rate observed in dynamic light scattering and the adoption of β-sheet structure indicated by CD and FTIR for these samples.

To examine the morphology of aggregates with arginine-containing compounds present, we imaged the samples by TEM. Aβ alone formed typical amyloid fibrils with a diameter of ~10 nm and lengths of up to 2 μm (Figure 7A). When Aβ was mixed with either ArgHCl or Arg, substantially longer fibrils were observed, especially in the case of Arg where in some cases no fibril ends were observed in many successive images (Figure 7B,C). These TEM observations confirmed results from light scattering, which

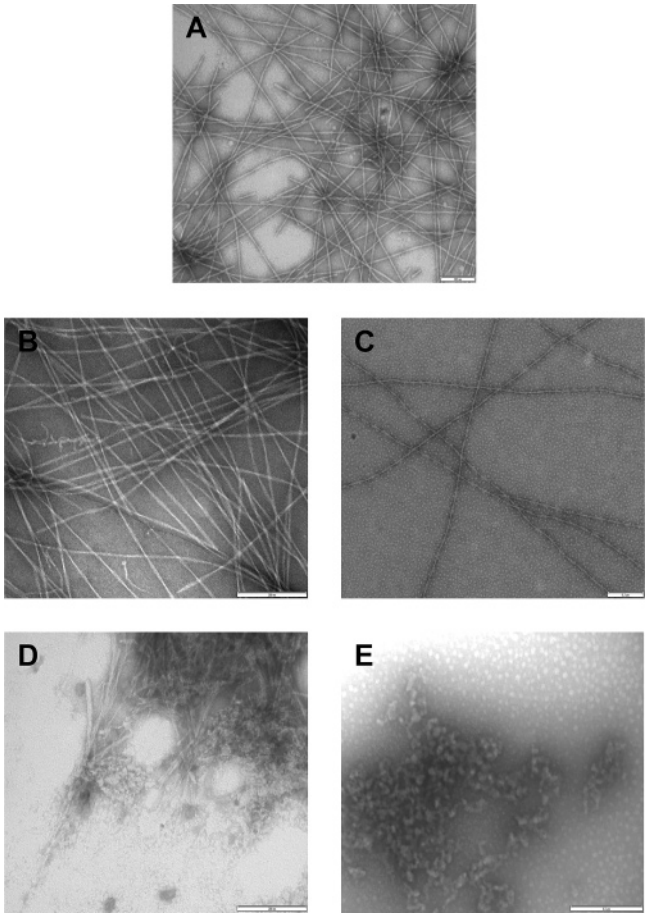

FIGURE 7: Aβ was dissolved in 8 M urea and then diluted 20-fold into PBSA (to a final concentration of 140 μM). (A) Aβ alone, (B) with 5700 μM ArgHCl, (C) with 5700 μM Arg, (D) with 140 μM RRRRRR, and (E) with 140 μM KLVFFRRRRRR. After 1−2 weeks of aggregation, samples were centrifuged, and the precipitated aggregates were collected, diluted, and vortexed. Samples were negatively stained and were placed on a pioloform coating grid support film for transmission electron microscopy imaging. The white bars represent 200 nm length.

indicated that samples of Aβ with Arg present contained fewer, longer aggregates than Aβ alone. The fibrils were very similar in diameter and general appearance to typical Aβ fibrils. In sharp contrast, RRRRRR and especially KLVFFRRRRRR produced a marked change in aggregate morphology despite minimal changes in CD and FTIR spectra. With RRRRRR present, fibrillar aggregates were still observed, but these tended to be much shorter and more clumped (Figure 7D). With KLVFFRRRRRR present, no aggregates with fibrillar morphology were observed; rather, large globular-like clumps of material were observed (Figure 7E). Thus, CD and FTIR indicated minimal secondary structural effects of KLVFFRRRRRR on Aβ, but TEM and light scattering both show very large effects on aggregate morphology and size.

In summary, arginine-containing compounds had very different effects on Aβ aggregation depending on the context in which arginine was presented. Arg monomer supports the formation of fewer, longer aggregates, as indicated by both light scattering and TEM results. Except for length, these aggregates are almost morphologically indistinguishable from Aβ fibrils, and there is little change in secondary structure of soluble or precipitated aggregates. With arginine hexamer in the disrupting domain of a hybrid compound (KLVFFRRRRRR), there were minimal changes in the secondary structure of soluble or precipitated Aβ, yet there was a significant acceleration in aggregation kinetics, resulting in the formation of clumpy aggregates packed so tightly that fibrillar morphology was no longer observable. These results show that arginine has drastic effects on the path of Aβ aggregation and that these effects are extremely different depending on the presentation context.

DISCUSSION

The Hofmeister series lists cosolutes according to their tendency to either stabilize (kosmotropic) or destabilize (chaotropic) protein structure (Figure 1). Kosmotropes stabilize proteins generally through their influence on the solvent (*15*, *16*). Nearly always, effective kosmotropes increase solvent surface tension (*17*, *18*). Kosmotropes are preferentially excluded from the protein surface, similar to their preferential exclusion from the air−solvent surface that results in increased surface tension (*15*, *27*, *30*). Preferential exclusion of cosolutes from the protein surface enhances hydrophobic interactions that drive the protein to its most structured (or compact) state.

With Aβ, the amyloid fibrillar aggregates are much more structured and compact than the natively disordered monomer. Hence, the acceleration of Aβ aggregation caused by our hybrid compounds may be best explained by the protein structure-stabilizing effect of Hofmeister kosmotropes. The increase in solvent surface tension of solutions of hybrid compounds correlated well with their ability to accelerate Aβ aggregation (*14*; Figure 3). This effect occurred when the disrupting domain of the hybrid compounds included moieties that have kosmotropic character, such as lysine, glutamic acid, and betaine.

KLVFFKKKKKK served as a base case for analysis of the influence of changes in the disrupting domain on activity. We first determined the effects of changes in the stereochemistry (KLVFFkkkkkk), side chain length (compound **5**), and geometry (compound **6**) of the disrupting domain. Compound **6** had very little effect on aggregation, compound **5** accelerated aggregation slightly, and KLVFFkkkkkk accelerated aggregation similar to KLVFFKKKKKK (Table 2, Figure 3). Hence, it is evident that there is significant importance in maintaining the straight chain orientation of the lysine disrupting domain, some importance in maintaining the side chain length, but very little importance in maintaining the L-amino acid stereochemistry. Interestingly, the varied effects of these compounds on aggregation correlated with their effects on solvent surface tension (Table 2, Figure 3), suggesting that solvent effects, rather than specific residue contacts between the disrupting domain and Aβ, are responsible for their effect on aggregation.

Although the sulfate group is generally an effective anionic kosmotrope (*16*), compound **2** was ineffective at accelerating Aβ aggregation. We considered two possible explanations for the lack of activity of compound **2**. One possibility is that the sulfate groups of compound **2** interact with specific sites on Aβ and, thus, cannot be preferentially excluded from the protein surface. This effect has been observed in several other cosolute/protein systems (*15*, *17*, *30*, *31*). Another explanation is that incorporating sulfate groups on the side chains of the disrupting domain does not provide the same

effect as free sulfate ions in solution. Although designed to contain a disrupting domain that mimics sulfates, compound **2** did not function as a kosmotrope, as witnessed by its lack of surface activity, and it had little effect on Aβ aggregation (Table 2, Figure 3). These results suggest that the surface tension effect is of greater importance than the chaotropic or kosmotropic classification of moieties incorporated into the disrupting domain.

Compounds **3** and **4** were investigated to determine if hybrid compounds could reduce surface tension and, thus, potentially decrease aggregation rate. The hydrocarbon nature of aminohexanoic acid (Ahx) and the PEG-like nature of aminoethoxyethoxyacetic acid (AEEA) suggested that there was potential for either or both of these compounds to decrease the solvent surface tension. The later elution time in reverse-phase HPLC purification of these two compounds indicated hydrophobic character (Figure 2). However, neither of these compounds had any significant effect on Aβ aggregation nor on the surface tension (Table 2, Figure 3).

Arginine is characterized by the Hofmeister series as a chaotrope (*16*) and has been utilized for suppression of protein aggregation during protein refolding (*21*−*26*, *30*). We wondered whether arginine, either alone or incorporated into a disrupting domain, would destabilize the folded amyloid fibril relative to the unfolded monomer and thereby reduce Aβ aggregation. Since chaotropic destabilization involves specific attractive interactions between the chaotrope and protein domains, the effect of a given chaotrope depends on the protein/peptide in question (*27*, *30*, *32*). Although arginine is classified as a Hofmeister chaotrope, the cosolute increases surface tension of aqueous solutions and stabilizes some proteins (*26*, *27*). Indeed, we observed that KLVFFR-RRRRR greatly enhanced Aβ aggregation and increased the solvent surface tension to levels nearly as high as compound **1** (Table 2, Figure 3). One explanation for the effect of KLVFFRRRRRR on Aβ aggregation is that arginine does not favorably associate with Aβ, so solvent effects dominate. Alternatively, it is also possible that arginine alone is chaotropic with Aβ but, when placed in the context of a multimeric disrupting-domain chain, it is not able to specifically interact with Aβ, again allowing the solvent effects to dominate.

In addition to KLVFFRRRRRR, we examined the influence of arginine and oligoarginine on Aβ aggregation. Results of our detailed analysis of the effects of the arginine-containing compounds may perhaps be best understood by considering the data in the context of a proposed kinetic model (*6*; Figure 8). Briefly, the model proposes that unstructured Aβ monomers ($M_{unfolded}$) quickly "refold" along two alternative pathways upon dilution into buffer at physiological pH. One path leads to formation of stable nonamyloidogenic monomers (M) and dimers (D), while the other path produces an amyloidogenic β-sheet intermediate (I). I self-associates into an oligomer (N), initiating filament (f) formation. I alternatively adds to the ends of N or to the ends of growing filaments in elongation steps. Since initiation is proposed to have a higher reaction order than elongation, the balance between initiation of new filaments vs filament growth is strongly concentration-dependent. Filaments are hypothesized to laterally align into fibrils (F) in a relatively slow step. Experimental support for this model has been published (*6*).

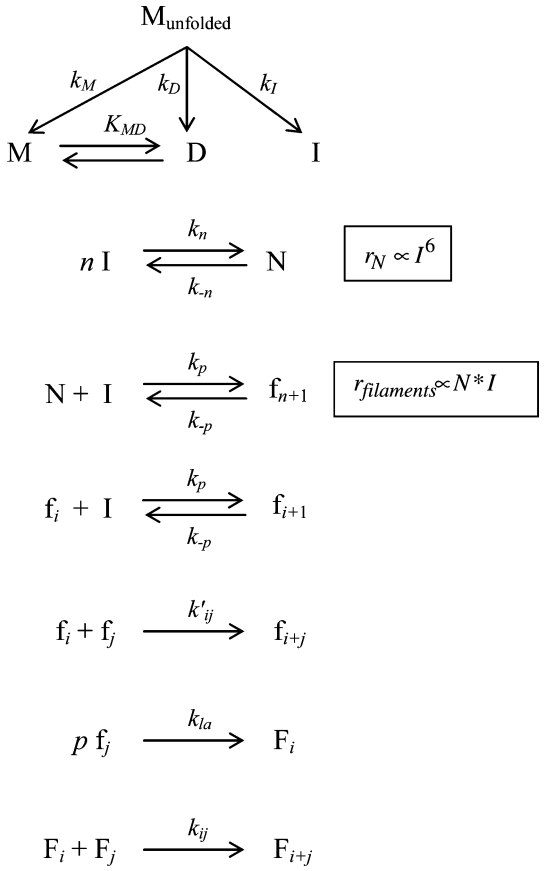

FIGURE 8: Simplified Aβ aggregation kinetic model (*6*).

Arg caused an increase in the hydrodynamic diameter of Aβ aggregates with a corresponding decrease in scattering intensity (Figure 4C,D), indicative of the formation of fewer, longer aggregate species. This finding was confirmed by TEM, where a few fibrils of indefinite lengths were observed (Figure 7C). If, indeed, initiation is a higher reaction order process than elongation, then the presence of fewer fibrils of increased length suggests that arginine reduces the fraction of Aβ participating in the amyloid pathway (Figure 8). Further support for this idea comes from the observation by FTIR of a minor loss in β-sheet structure of precipitated material with Arg present and the qualitative observation that there was less visible precipitate with Arg present.

Since the alkaline nature of Arg increased the buffer pH (from 7.4 to 9.0), we also tested ArgHCl for its effect on Aβ aggregation. ArgHCl also caused a decrease in scattered light intensity (observable after 15−20 h), although its effects were mild compared to Arg. Similar to Arg, ArgHCl caused a slight loss in β-sheet structure of precipitated material and resulted in less visible precipitate after several weeks of aggregation.

RRRRRR accelerated Aβ aggregation, but not nearly as much as KLVFFRRRRRR (Figure 4A,B). Here we are most likely seeing activity from the effects on solvent properties (similar to what we have speculated for KLVFFRRRRRR), but the effect is extremely diminished without KLVFF present. We hypothesize that the binding capability of KLVFF allows Aβ to experience a more significant change in solvent properties because of the localization of the compound. Indeed, KLVIIKKKKKK increased solvent surface tension but had little or no effect on Aβ aggregation (data not shown), and KLVII unlike KLVFF has no binding

affinity for Aβ (*30*), demonstrating the important contribution of the recognition domain.

KLVFFRRRRRR and RRRRRR, in addition to accelerating the rate of Aβ aggregation, produced morphologically distinct aggregates (Figure 7D,E); RRRRRR plus Aβ produced aggregates that appear by TEM to be clumps of short fibrils, while KLVFFRRRRRR plus Aβ aggregates had an amorphous appearance. However, there was very little change in secondary structure of either soluble or precipitated aggregates; the apparent minor degree of structural loss evident in CD for both of these compounds (Figure 5) is most likely attributed to contribution to the signal from the unstructured backbone of KLVFFRRRRRR or RRRRRR. The observed effects could be a result of extensive lateral packing of aggregates with β-sheet structure. An increased rate of lateral association (relative to elongation) of filaments would produce stacks of shorter, thicker fibrils, which could result in aggregates that have more of the observed clumpy morphology instead of the typical fibril-like morphology. This extreme packing could have the effect of burying β-sheet domains that would normally be exposed in individual fibrils, causing the domains to be excluded from ThT binding; such behavior could explain the lack of ThT fluorescence with RRRRRR or KLVFFRRRRRR present (Figure 6). Together, these results suggest that these two compounds may affect later stages of the aggregation process, increasing the kinetics of lateral association (k_{la}) of filaments into fibrils (Figure 8) but not altering the fraction of β-sheet material participating in the amyloid pathway.

The proposed effect of KLVFFRRRRRR and RRRRRR on later stages of the Aβ aggregation process is similar to the effect observed for KLVFFKKKKKK, which was shown to influence Aβ aggregation by increasing k_{la} (*33*; Figure 8). Of these three compounds, only KLVFFKKKKKK contains a disrupting domain that is characterized as a Hofmeister kosmotrope; however, all of these compounds share the common characteristic of increasing solvent surface tension, and it seems that this effect governs their influence on aggregation. This solvent effect is known to stabilize structured protein by enhancing hydrophobic interactions (*15*), and hydrophobic interactions are most essential in driving lateral association of Aβ aggregates. In contrast, the effect of monomeric arginine is most likely attributed to chaotropic protein binding interactions. It is likely that binding and destabilization occur at initial aggregate stages, reducing the amount of amyloidogenic Aβ that can further proceed to form fibrils.

Compounds with arginine presented in different contexts influenced Aβ aggregation in strikingly different ways. An interpretation of the differences was only possible by analysis of aggregation with several techniques. For example, if the ThT assay alone was used to measure the effect of RRRRRR or KLVFFRRRRRR on Aβ aggregation, one might conclude that these compounds inhibit Aβ aggregation. However, light scattering and TEM demonstrated that, in fact, Aβ is significantly aggregated in the presence of these compounds. Hence this study demonstrates the benefits of using multiple techniques to analyze protein/peptide aggregation characteristics.

This work may be relevant to other protein folding/aggregating systems. Using the strategy outlined here, it may be possible to develop a general approach toward designing compounds that alter protein folding/aggregation by specifically targeting protein domains with a recognition domain and incorporating surface tension modifying elements in the disrupting domain.

ACKNOWLEDGMENT

Peptides were synthesized at the University of Wisconsin—Madison Biotechnology Center with help from Dr. Gary Case. Dr. Martha Vestling provided MALDI mass spectrometry analysis. CD data were obtained at the University of Wisconsin—Madison Biophysics Instrumentation Facility, supported by National Science Foundation Grants BIR-9512577 and S10RR13790. Dr. Andrew Tseng assisted with collection of FTIR data. TEM imaging was performed by Randall J. Massey at the University of Wisconsin Medical Sciences Center. We thank Dr. Jin Kim for assistance with experiments and helpful discussions.

REFERENCES

1. Pike, C. J., Burdick, D., Walencewicz, A. J., and Glabe, C. W. (1993) Neurodegeneration induced by beta-amyloid peptides in vitro: the role of peptide assembly state, *J. Neurosci. 13*, 1676−1687.
2. Simmons, L. K., May, P. C., Tomaselli, K. J., Rydel, R. E., Fuson, K. S., Brigham, E. F., Wrigth, S., Lieberburg, I., Becker, G. W., and Brems, D. N. (1994) Secondary structure of amyloid beta peptide correlates with neurotoxic activity in vitro, *Mol. Pharmacol. 45*, 373−379.
3. Seilheimer, B., Bohrmann, B., Bondolfi, L., Muller, F., Stuber, D., and Dobeli, H. (1997) The toxicity of the Alzheimer's beta-amyloid peptide correlates with a distinct fiber morphology, *J. Struct. Biol. 119*, 59−71.
4. Hardy, J., and Selkoe, D. J. (2002) The amyloid hypothesis of Alzheimer's disease: progress and problems on the road to therapeutics, *Science 297*, 353−356.
5. Kayed, R., Head, E., Thompson, J. L., McIntire, T. M., Milton, S. C., Cotman, C. W., and Glabe, C. G. (2003) Common structure of soluble amyloid oligomers implies common mechanism of pathogenesis, *Science 300*, 486−489.
6. Pallitto, M. M., and Murphy, R. M. (2001) A mathematical model of the kinetics of beta-amyloid fibril growth from the denatured state, *Biophys. J. 81*, 1805−1822.
7. Roher, A. E., Chany, M. O., Kuo, Y. M., Webster, S. D., Stine, W. B., Haverkamp, L. J., Woods, A. S., Cotter, R. J., Tuohy, J. M., Kraft, G. A., Bonnell, B. S., and Emmerling, M. R. (1996) Morphology and toxicity of Abeta-(1−42) dimer derived from neuritic and vascular amyloid deposits of Alzheimer's disease, *J. Biol. Chem. 271*, 20631−20635.
8. Lambert, M. P., Barlow, A. K., Chromy, B. A., Edwards, C., Freed, R., Liosatos, M., Morgan, T. E., Rozovsky, I., Trommer, B., Viola, K. L., Wals, P., Zhang, C., Finch, C. E., Kraft, G. A., and Klein, W. L. (1998) Diffusible, nonfibrillar ligands derived from Abeta1−42 are potent central nervous system neurotoxins, *Proc. Natl. Acad. Sci. U.S.A. 95*, 6448−6453.
9. Hartley, D. M., Walsh, D. M., Ye, C. P., Diehl, T., Vasquez, S., Vassilev, P. M., Teplow, D. B., and Selkoe, D. J. (1999) Protofibrillar intermediates of amyloid beta-protein induce acute electrophysiological changes and progressive neurotoxicity in cortical neurons, *J. Neurosci. 19*, 8876−8884.
10. Ward, R. V., Jennings, K. H., Jepras, R., Neville, W., Owen, D. E., Hawkins, J., Christie, G., Davis, J. B., George, A., Karran, E. H., and Howlett, D. R. (2000) Fractionation and characterization of oligomeric, protofibrillar and fibrillar forms of beta-amyloid peptide, *Biochem. J. 348* (Part 1), 137−144.
11. Ghanta, J., Shen, C. L., Kiessling, L. L., and Murphy, R. M. (1996) A strategy for designing inhibitors of beta-amyloid toxicity, *J. Biol. Chem. 271*, 29525−29528.
12. Pallitto, M. M., Ghanta, J., Heinzelman, P., Kiessling, L. L., and Murphy, R. M. (1999) Recognition sequence design for peptidyl modulators of beta-amyloid aggregation and toxicity, *Biochemistry 38*, 3570−3578.
13. Lowe, T. L., Strzelec, A., Kiessling, L. L., and Murphy, R. M. (2001) Structure−function relationships for inhibitors of beta-

amyloid toxicity containing the recognition sequence KLVFF, *Biochemistry 40*, 7882−7889.
14. Kim, J. R., Gibson, T. J., and Murphy, R. M. (2003) Targeted control of kinetics of beta-amyloid self-association by surface tension-modifying peptides, *J. Biol. Chem. 278*, 40730−40735.
15. Neagu, A., Neagu, M., and Der, A. (2001) Fluctuations and the Hofmeister effect, *Biophys. J. 81*, 1285−1294.
16. Cacace, M. G., Landau, E. M., and Ramsden, J. J. (1997) The Hofmeister series: salt and solvent effects on interfacial phenomena, *Q. Rev. Biophys. 30*, 241−277.
17. Lin, T. Y., and Timasheff, S. N. (1996) On the role of surface tension in the stabilization of globular proteins, *Protein Sci. 5*, 372−381.
18. Soderlund, T., Alakoskela, J. M., Pakkanen, A. L., and Kinnunen, P. K. (2003) Comparison of the effects of surface tension and osmotic pressure on the interfacial hydration of a fluid phospholipid bilayer, *Biophys. J. 85*, 2333−2341.
19. Shiraki, K., Kudou, M., Fujiwara, S., Imanaka, T., and Takagi, M. (2002) Biophysical effect of amino acids on the prevention of protein aggregation, *J. Biochem. 132*, 591−595.
20. Shiraki, K., Kudou, M., Nishikori, S., Kitagawa, H., Imanaka, T., and Takagi, M. (2004) Arginine ethylester prevents thermal inactivation and aggregation of lysozyme, *Eur. J. Biochem. 271*, 3242−3247.
21. Xie, Q., Guo, T., Lu, J., and Zhou, H. M. (2004) The guanidine like effects of arginine on aminoacylase and salt-induced molten globule state, *Int. J. Biochem. Cell Biol. 36*, 296−306.
22. Qiao, Z. S., Guo, Z. Y., and Feng, Y. M. (2001) Putative disulfide-forming pathway of porcine insulin precursor during its refolding in vitro, *Biochemistry 40*, 2662−2668.
23. Buchner, J., and Rudolph, R. (1991) Renaturation, purification and characterization of recombinant Fab-fragments produced in *Escherichia coli*, *Bio/Technology 9*, 157−162.
24. Arakawa, T., and Tsumoto, K. (2003) The effects of arginine on refolding of aggregated proteins: not facilitate refolding, but suppress aggregation, *Biochem. Biophys. Res. Commun. 304*, 148−152.
25. Taneja, S., and Ahmad, F. (1994) Increased thermal stability of proteins in the presence of amino acids, *Biochem. J. 303* (Part 1), 147−153.
26. Tsumoto, K., Umetsu, M., Kumagai, I., Ejima, D., Philo, J. S., and Arakawa, T. (2004) Role of arginine in protein refolding, solubilization, and purification, *Biotechnol. Prog. 20*, 1301−1308.
27. Kita, Y., Arakawa, T., Lin, T. Y., and Timasheff, S. N. (1994) Contribution of the surface free energy perturbation to protein−solvent interactions, *Biochemistry 33*, 15178−15189.
28. Bouchard, M., Zurdo, J., Nettleton, E. J., Dobson, C. M., and Robinson, C. V. (2000) Formation of insulin amyloid fibrils followed by FTIR simultaneously with CD and electron microscopy, *Protein Sci. 9*, 1960−1967.
29. Halverson, K., Fraser, P. E., Kirschner, D. A., and Lansbury, P. T., Jr. (1990) Molecular determinants of amyloid deposition in Alzheimer's disease: conformational studies of synthetic beta-protein fragments, *Biochemistry 29*, 2639−1644.
30. Arakawa, T., Bhat, R., and Timasheff, S. N. (1990) Why preferential hydration does not always stabilize the native structure of globular proteins, *Biochemistry 29*, 1924−1931.
31. Record, M. T., Jr., Zhang, W., and Anderson, C. F. (1998) Analysis of effects of salts and uncharged solutes on protein and nucleic acid equilibria and processes: a practical guide to recognizing and interpreting polyelectrolyte effects, Hofmeister effects, and osmotic effects of salts, *Adv. Protein Chem. 51*, 281−353.
32. Breslow, R., and Guo, T. (1990) Surface tension measurements show that chaotropic salting-in denaturants are not just water-structure breakers, *Proc. Natl. Acad. Sci. U.S.A. 87*, 167−169.
33. Kim, J. R., and Murphy, R. M. (2004) Mechanism of accelerated assembly of beta-amyloid filaments into fibrils by KLVFFK(6), *Biophys. J. 86*, 3194−3203.
34. Shen, C. L., Scott, G. L., Merchant, F., and Murphy, R. M. (1993) Light scattering analysis of fibril growth from the amino-terminal fragment beta(1−28) of beta-amyloid peptide, *Biophys. J. 65*, 2383−2395.

BI050225S